

# Role of the van der Waals interactions on the bonding mechanism of pyridine on Cu(110) and Ag(110) surface: First-principles study

N. Atodiresei,<sup>1,2,\*</sup> V. Caciuc,<sup>3</sup> J.-H. Franke,<sup>3</sup> and S. Blügel<sup>1</sup><sup>1</sup>*Institut für Festkörperforschung (IFF), Forschungszentrum Jülich, 52425 Jülich, Germany*<sup>2</sup>*The Institute of Scientific and Industrial Research, Osaka University, 8-1 Mihogaoka, Ibaraki Osaka, 567-0047 Japan*<sup>3</sup>*Physikalisches Institut, Westfälische Wilhelms Universität Münster, Wilhelm-Klemm-Strasse 10, 48149 Münster, Germany*

(Received 2 April 2008; revised manuscript received 11 June 2008; published 10 July 2008)

We performed density-functional calculations aimed to investigate the adsorption mechanism of a single pyridine ( $C_5H_5N$ ) molecule on Cu(110) and Ag(110) surfaces. Our *ab initio* simulations show that, in the ground state, the pyridine molecule adsorbs with its molecular plane perpendicular to these substrates and is oriented along the [001] direction. In this case, the bonding mechanism involves a  $\sigma$  bond through the lone-pair electrons of the nitrogen atom. When the heterocyclic ring is parallel to the surface, the bonding takes place via  $\pi$ -like molecular orbitals. However, depending on the position of the N atom on the surface, the planar adsorption configuration can relax to a perpendicular geometry. The role of the long-range van der Waals interactions on the adsorption geometries and energies was analyzed in the framework of the semiempirical method proposed by Grimme [J. Comput. Chem. **27**, 1787 (2006)]. We demonstrate that these dispersion effects are very important for geometry and electronic structure of flat adsorption configurations.

DOI: [10.1103/PhysRevB.78.045411](https://doi.org/10.1103/PhysRevB.78.045411)

PACS number(s): 68.43.Bc, 71.15.Mb, 68.43.Fg

## I. INTRODUCTION

To surpass the intrinsic size limits of the silicon-based electronic devices, the coupling between the molecular and the macroscopic world is at the moment one of the most important perspective. The ultimate goal of this approach is to construct devices in which the adsorbed organic molecules on surfaces are the main functional units.<sup>1</sup> Among the advantages of using molecules in future electronic devices, it is worth mentioning the possibility of designing such devices at a molecular scale to construct organic field-effect transistors<sup>2-4</sup> or ultrahigh-density memory circuits.<sup>5</sup>

A promising way to manufacture a molecular electronic device is to use self-assembled monolayers (SAM)<sup>6</sup> adsorbed on a specific substrate. This approach was employed, for instance, to study several thiolate SAMs on gold surfaces (see, for instance, Refs. 7-9). Single molecules with thiol ends were also used to construct single-atom transistors.<sup>10</sup> To elucidate the electronic structure of certain thiol-based SAM-substrate interfaces, several theoretical studies were performed.<sup>11-13</sup> In particular, these *ab initio* simulations clearly emphasized that the electronic properties of a SAM-surface system depend on a delicate balance between molecule-molecule and molecule-substrate interactions.

Less investigated are systems where the binding atom between the molecules and surfaces is not a sulfur or an oxygen atom (as a part, for instance, of a carboxylate anchoring group<sup>14-16</sup>). Therefore, in the present study we focus on the bonding mechanism of a single pyridine molecule adsorbed via its nitrogen atom on Ag(110) and Cu(110) surfaces. Our interest to analyze the behavior of a single molecule is basically motivated by the need to separate the two above mentioned competing interactions present in a SAM. For a metallic surface, the adsorption process of a single pyridine molecule was investigated from first-principles for Au(111) (Ref. 17) and Cu(100) (Ref. 18) substrates. In particular, the specific nature of the molecule-surface bonding mechanism

(physisorption or chemisorption) is the key factor, which largely determines the characteristics of a molecular-based electronic device.

The adsorption process of pyridine ( $C_5H_5N$ ) as a function of temperature and coverage was experimentally studied for several metal surfaces (see, for instance, Ref. 19 and the references cited therein). The peculiar feature of this molecule is the possibility to interact with the substrate: (i) via its planar aromatic  $\pi$ -like molecular orbital in a similar fashion to benzene ( $C_6H_6$ ) on Cu(110) surface<sup>20,21</sup> or/and (ii) through its nitrogen lone-pair electrons. In the first case the pyridine adsorbs with its molecular plane parallel to surface, while in the second case the heterocyclic ring is perpendicular to surface. At low coverage, the competition between these two adsorption mechanisms might lead to a planar, tilted, or perpendicular binding geometries as well as a mixture of them.

Remarkably, in the case of pyridine on Ag(110) surface a recent low-temperature scanning tunneling microscopy (STM) investigation<sup>22</sup> showed that the isolated molecule binds to this surface only through the nitrogen lone-pair electrons. Similarly, the electron stimulated desorption ion angular distribution (ESDIAD) studies<sup>23,24</sup> of the isolated pyridine on Cu(110) surface also revealed a perpendicular adsorption geometry. In these studies it was assumed that the heterocyclic ring is oriented along the [001] direction of the (110) surface. Another possible orientation of the molecular plane is along the  $[1\bar{1}0]$  direction or it can be even twisted between these two directions. However, the STM study<sup>19</sup> of  $C_5H_5N$  on the Cu(110) surface suggested also the presence of a tilted adsorption geometry in the limit of a very low coverage. In this peculiar case, the adsorption process involves both the nitrogen lone-pair and  $\pi$ -like molecular orbitals.

Since the bulk structure of both metals is face-centered cubic (fcc), an upright binding geometry of pyridine on the (110) surface suggests a similar interaction pattern of this molecule with the substrates under consideration. In this con-

text, it is interesting to analyze how the relative position of the  $d$  band of the Cu(110) and Ag(110) surfaces with respect to their Fermi level changes the physical properties of the molecule-substrate interface. Therefore, in the present study we focused on the bonding mechanism of pyridine on these surfaces by performing *ab initio* simulations. To elucidate the role of the orientation of the molecular plane on the adsorption process, we considered several adsorption geometries with the heterocyclic ring parallel or perpendicular to substrates. The relevance of long-range van der Waals interactions on the molecule-surface adsorption process was investigated by means of a semiempirical approach. The total-energy calculations showed that in the ground-state adsorption configuration of pyridine on Cu(110) and Ag(110) surfaces, the heterocyclic ring is indeed perpendicular to these substrates and oriented along the [001] direction. In general, the van der Waals interactions are more important for the parallel adsorption configurations than for the perpendicular ones. From electronic point of view, the binding of  $C_5H_5N$  on these surfaces is governed by a strong hybridization of the highest occupied molecular orbital (HOMO) with the  $d$  band of the substrates. Interestingly, on both substrates the lowest unoccupied molecular orbital (LUMO) does not participate to the bonding mechanism.

## II. THEORETICAL METHOD

To analyze the physical properties of the pyridine-metal surface interface we performed first-principles total-energy calculations based on the density-functional theory (DFT) (Ref. 25) in a pseudopotential plane-wave implementation as provided by the VASP code.<sup>26,27</sup> The electron-ion interactions were taken into account by pseudopotentials generated using the projector augmented wave (PAW) method.<sup>28,29</sup> For the exchange-correlation energy functional we employed the generalized gradient approximation (GGA) as parameterized by Perdew *et al.*<sup>30</sup> [Perdew Burke Ernzerhof (PBE) energy functional].

The molecule-metal system was modeled by a repeated slab consisting of five atomic layers separated by a vacuum region of  $\approx 16$  Å. We checked the consistency of our results by using seven and nine atomic layers, respectively. A single pyridine molecule was adsorbed on one side of the slab. To avoid the interactions between a molecule and its periodically repeated images, a  $4 \times 5$  in-plane surface unit cell for the Cu(110) and Ag(110) surfaces was utilized. The (110) surfaces of these metals were generated using the theoretical lattice parameters calculated for the bulk copper (3.636 Å) and silver (4.165 Å), respectively. The geometry of the pyridine-(110) metal surface was optimized by relaxing all molecule atoms and those of the two surface layers. The corresponding relaxed geometries were obtained when the calculated Hellmann-Feynman forces were smaller than  $\approx 0.001$  eV/Å. To calculate such accurate forces, the plane-wave basis set included all plane waves up to a cutoff energy  $E_{\text{cut}}$  of 450.0 eV. Due to the large size of the supercells used in our *ab initio* simulations, the Brillouin zone was sampled by the  $\Gamma$  point only. Besides this, our calculations were dipole corrected by using a dipole sheet in the middle of the vacuum slab.<sup>31</sup>

To investigate the structural stability of the pyridine on the Cu(110) and Ag(110) surfaces, we focused mainly on two different perpendicular adsorption configurations determined by a parallel orientation of the molecular plane to the [001] (hereafter denoted as [001] adsorption geometry) and  $[1\bar{1}0]$  (hereafter denoted as  $1\bar{1}0$  adsorption geometry) crystallographic directions. Besides these, perpendicular geometries we also considered several parallel adsorption configurations such that the molecular plane is parallel to Cu(110) and Ag(110) surfaces. The relative stability of these adsorption geometries can be assessed from the calculated adsorption energy  $E_{\text{ads}}$  defined as

$$E_{\text{ads}} = E_{\text{sys}} - E_{\text{pyridine}} - E_{(\text{Cu,Ag})(110)}, \quad (1)$$

where  $E_{\text{sys}}$  represents the total energy of the relaxed pyridine-(110) metal surface system,  $E_{\text{pyridine}}$  is the total energy of the isolated pyridine molecule, and  $E_{(\text{Cu,Ag})(110)}$  are the total energies of the isolated Cu(110) and Ag(110) surfaces, respectively.

A final note concerns the role of the long-range van der Waals interactions on the geometry and adsorption energy of the pyridine-metal system. In the present study we considered these effects by employing the semiempirical approach proposed by Grimme.<sup>32</sup> This method relies on corrections added to the DFT-GGA total energy and forces derived from a damped atom-pairwise potential  $C_6 R^{-6}$  ( $C_6$  represents the dispersion coefficient for a given atom pair and  $R$  is the distance between the atoms). The self-consistent calculated van der Waals energy and forces were then used during the structural relaxations of the pyridine on metal surfaces under consideration. Notice that the semiempirical method employed in our study to account for the van der Waals interactions is similar to that developed by Ortman *et al.*<sup>33,34</sup> and used, for instance, to investigate the adsorption of adenine on graphite(0001) surface.<sup>33</sup>

## III. RESULTS AND DISCUSSION

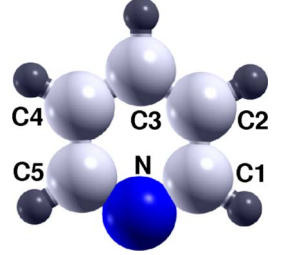
### A. Pyridine in gas phase

As a preliminary step of our study, we optimized the geometry of the pyridine molecule in the gas phase using an orthorhombic supercell with dimensions of  $20 \times 20 \times 20$  Å<sup>3</sup>. The calculated bond lengths and bond angles are presented in Table I and are in a very good agreement with the experimental data published in Ref. 35. For comparison, in this table we also list the similar theoretical values obtained by means of *ab initio* Hartree-Fock (HF) (Refs. 36 and 37) and DFT (Ref. 17) methods. While the DFT and HF bond lengths are almost the same, it seems that the HF method slightly overestimates the bond angles, most notably for the bond angle determined by the N, C1, and C5 atoms ( $\approx 2^\circ$ ).

Since the basic goal of our study is to investigate how the electronic structures of the pyridine and metal surface change due to their interaction, in Fig. 5(a) we present the angular-momentum resolved local density of states (LDOS) calculated for the  $C_5H_5N$  molecule in the gas phase. Of particular interest are the frontier orbitals, namely, the highest occupied molecular orbitals (HOMOs:  $\pi_2$ ,  $\pi_1$ , and  $\sigma$ ) and lowest un-

TABLE I. (Color online) The bond lengths and bond angles calculated for the pyridine molecule in gas phase and adsorbed on Cu(110) and Ag(110) surfaces. Note that in the case of the adsorbed pyridine molecule, only the data for the ground-state adsorption geometry (the molecular plane is perpendicular to surface and oriented along the [001] surface direction) and those of the most stable parallel adsorption configuration are reported.

	Gas phase				Cu(100)		Ag(110)	
	This work	Ref. <a href="#">35</a>	Ref. <a href="#">36</a>	Ref. <a href="#">17</a>	[001]	Flat	[001]	Flat
Bond length (Å)								
N-C1	1.343	1.338	1.338	1.340	1.351	1.344	1.346	1.343
N-C5	1.343	1.338	1.338	1.340	1.351	1.344	1.346	1.343
C1-C2	1.398	1.394	1.395	1.394	1.391	1.410	1.394	1.401
C2-C3	1.396	1.392	1.395	1.391	1.396	1.412	1.396	1.398
C3-C4	1.396	1.392	1.395	1.391	1.396	1.412	1.396	1.398
C4-C5	1.398	1.394	1.395	1.394	1.391	1.410	1.394	1.401
N-Metal	-	-	-	-	2.022	2.488	2.348	2.516
C2 (C4)-Metal	-	-	-	-	2.116	2.305	2.439	3.015
Bond angle (deg)								
C1-N-C5	117.1	116.9	118.8	117.1	118.2	117.5	118.4	117.9
N-C1-C2	123.7	123.8	122.6	123.5	122.6	123.0	122.6	123.0
C1-C2-C3	118.5	118.5	118.5	118.4	119.1	119.0	118.8	118.8



Atomic labels of the pyridine molecule

occupied molecular orbitals (LUMOs:  $\pi_1^*$  and  $\pi_2^*$ ). The Cartesian coordinate system was chosen such that the  $p_x$  and  $p_y$  atomic orbitals are *in* the molecular plane while the  $p_z$  orbital is oriented *perpendicular* to it.

With this specification the HOMO is a  $\sigma$  in-plane molecular orbital, because it consists of a combination of  $s$ ,  $p_x$ , and  $p_y$  atomic orbitals, while the LUMO ( $\pi_2^*$ ) is a  $\pi$  molecular orbital since it originates from a  $p_z$  atomic orbitals perpendicular to the molecular plane. Note that the bonding orbitals HOMO-1( $\pi_1$ ), HOMO-2( $\pi_2$ ), and the antibonding one LUMO+1( $\pi_2^*$ ) also have a  $\pi$  character. Since the spatial distribution of the charge density corresponding to these molecular orbitals and their nodal structure are key factors in describing the interaction of pyridine with surfaces, in Fig. 1 we present the charge-density plots of  $\pi_2$ ,  $\pi_1$ ,  $\sigma$ ,  $\pi_1^*$ , and  $\pi_2^*$  orbitals [see also Fig. 5(a)]. Note the accumulation of charge density around the N atom in the case of HOMO and the presence of a nodal plane in the molecular plane in the case of HOMO-2, HOMO-1, LUMO, and LUMO+1. The relevance of these features on the mechanism of the pyridine adsorption on the studied metallic surfaces will be emphasized later.

### B. Ground-state geometry and energetics

As mentioned in Sec. I, the pyridine molecule can adsorb on surfaces with its molecular plane perpendicular or parallel to the substrate under consideration. In the former case the adsorption process involves the nitrogen lone-pair electrons ( $\sigma$ -like molecular orbital), while in the latter case it is due to the  $\pi$ -like molecular orbital. Another possibility is represented by a tilted adsorption geometry which implies the presence of both lone-pair and  $\pi$ -like interactions with the surface. On the Ag(110) surface, the isolated  $C_5H_5N$  molecule adsorbs via its nitrogen lone-pair orbital.<sup>22</sup> Similarly, in

the case of the Cu(110) surface, some experimental studies<sup>23,24</sup> suggest also a perpendicular adsorption geometry even if a tilted configuration cannot be ruled out.<sup>19</sup> Therefore, in this section we analyze the strength of the pyridine-substrate interaction when the molecular plane is oriented perpendicular or parallel to the surface.

The calculated adsorption energies  $E_{\text{ads}}$  of a single pyridine molecule on the Cu(110) and Ag(110) surfaces are reported in Table II. The analysis of these values clearly shows that for both surfaces, the perpendicular adsorption configuration corresponding to the molecular plane aligned parallel to the [001] direction is the ground-state geometry (see Fig. 2). A larger adsorption energy calculated for the  $C_5H_5N$  on the Cu(110) surface than that obtained when it is adsorbed on the Ag(110) one suggests a stronger molecule-substrate interaction in the former case. This behavior can be traced back to a different strength of the hybridization between the HOMOs

TABLE II. The adsorption energies  $E_{\text{ads}}$  of the pyridine molecule on Cu(110) and Ag(110) calculated for the most stable perpendicular and parallel (flat) adsorption geometries.  $E_{\text{ads}}^{\text{PBE}}$  refers to the adsorption energies obtained without van der Waals corrections and  $E_{\text{ads}}^{\text{PBE+vdW}}$  to those calculated with a van der Waals-corrected energy functional (Ref. [32](#)).

Surface	Orientation	Adsorption energy	
		$E_{\text{ads}}^{\text{PBE}}$ (eV)	$E_{\text{ads}}^{\text{PBE+vdW}}$ (eV)
Cu(110)	[001]	-0.758	-0.972
	[1 $\bar{1}$ 0]	-0.629	-0.842
	flat	-0.108	-0.522
Ag(110)	[001]	-0.447	-0.595
	[1 $\bar{1}$ 0]	-0.381	-0.573
	flat	-0.084	-0.369





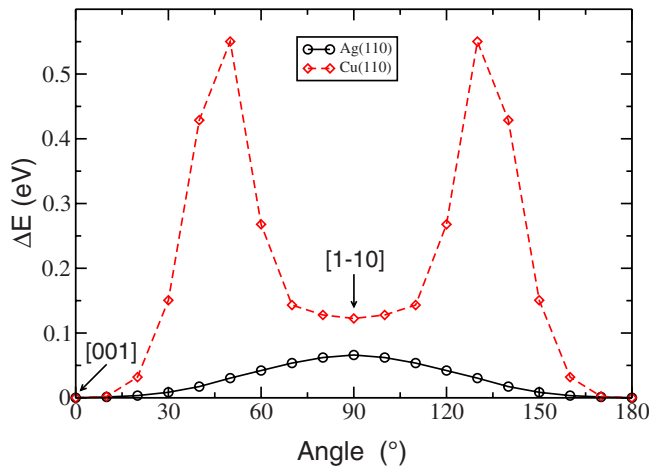


FIG. 3. (Color online) Potential energy barriers obtained by rotating the pyridine on Cu(Ag)(110) surface from [001] to  $[1\bar{1}0]$  adsorption configuration. At each rotation step the pyridine-substrate geometries were relaxed in a direction perpendicular to the surface. Characteristic of the Ag(110) surface is a smooth energetic transition when rotating the molecular ring from the [001] to  $[1\bar{1}0]$  direction (continuous line and open circles). On the contrary, for the Cu(110) surface the  $[1\bar{1}0]$  adsorption configuration is a local minimum separated by an energy barrier of  $\approx 0.55$  eV from the ground-state [001] geometry (dotted line and open squares).

adsorption configuration is a local minimum separated by an energy barrier of  $\approx 0.55$  eV from the [001] adsorption geometry.

It is interesting to note that, starting with an initially flat geometry of pyridine on the Cu(110) and Ag(110) substrates, the geometry of the final relaxed configuration sensitively depends on the position of the N atom on the surface. As presented in Figs. 4(a)–4(c), when the N atom is placed close to a surface atom or above it, the molecule-substrate interactions lead to a relaxed geometry with the heterocyclic ring *perpendicular* to the surface [see Fig. 4(d)]. In comparison to the ground-state geometry, this adsorption configuration has the molecular plane twisted with an angle of  $\approx 21.7^\circ$  with respect to the [001] direction. Such an adsorption geometry is similar to that obtained for the Cu(100) surface;<sup>18</sup> however, in the latter case it represents the ground-state configuration. The lift of the molecular plane from a parallel to a perpendicular adsorption geometry evidenced in our *ab initio* study is a clear fingerprint of a competition between the  $\sigma$ - and  $\pi$ -like interactions of the pyridine molecule with the Cu(110) and Ag(110) surfaces.

However, when the N atom lies between the surface atoms [see Figs. 4(e)–4(g)], the pyridine molecule relaxes to a geometry with the molecular plane almost parallel to the Cu(110) and Ag(110) surfaces. In the most stable flat configuration depicted in Fig. 4(g), the average vertical distance between the molecule and the surface atoms is  $\approx 3.0$  Å in the case of the Cu(110) substrate and  $\approx 3.2$  Å for the Ag(110) one. An additional difference consists in a slightly larger angle between the molecular plane and the Ag(110) surface ( $\approx 9^\circ$ ) than that on the Cu(110) one ( $\approx 3^\circ$ ).

### C. Role of the van der Waals interactions on the ground-state geometry

A flat adsorption geometry of the pyridine molecule on the Cu(110) and Ag(110) substrates with an averaged molecule-surface distance of  $\approx 3.0$  Å and  $\approx 3.25$  Å raises the question of what is the relevance of the long-range van der Waals interactions on the calculated geometry and adsorption energies. In particular, the van der Waals interactions are important when a molecule adsorbs through a  $\pi$ -like molecular orbital and this is exactly the case of a parallel adsorption geometry of pyridine on these surfaces. In consequence, we performed structural relaxations for several parallel and perpendicular adsorption geometries taking into account the long-range van der Waals forces.<sup>32</sup>

The relaxed geometry of the pyridine molecule in the perpendicular adsorption configurations obtained with the inclusion of the van der Waals forces is basically the same as without considering these forces. However, a van der Waals-corrected energy functional (PBE+vdW) leads to lower adsorption energy of  $\approx 0.2$  eV for both surfaces (see Table I). It is interesting to note that, although these corrections are semiempirical, the calculated van der Waals-corrected adsorption energy for  $C_5H_5N$  on Cu(110) surface in its ground state is  $\approx -0.97$  eV, which is essentially the same with the experimental value reported in Ref. 23.

For the parallel adsorption configurations the van der Waals corrections are important from both geometrical and energetic point of views. Since the long-range van der Waals forces are attractive, the geometrical effect is to bring the pyridine molecule closer to a surface. Indeed, the average vertical molecule-surface distance is now  $\approx 2.4$  Å on Cu(110) surface and  $\approx 2.9$  Å on Ag(110) one. The angle between the molecular plane and the metal surfaces also slightly increases from  $\approx 3^\circ$  to  $\approx 7^\circ$  for  $C_5H_5N$  on Cu(110) and from  $\approx 9^\circ$  to  $\approx 14^\circ$  on the Ag(110) surface. Besides these geometrical effects, the inclusion of the van der Waals interactions has a substantial effect on the adsorption energies. For instance, the PBE+vdW functional corrects the DFT value of the adsorption energy for pyridine on Cu(110) surface from  $\approx -0.21$  to  $\approx -0.61$  eV (the energy gain is  $\approx -0.40$  eV) and from  $\approx -0.08$  to  $\approx -0.37$  eV (the energy gain is  $\approx -0.30$  eV) on Ag(110) substrate (see Table I). Note also that these van der Waals energy corrections are larger for Cu(110) surface than for Ag(110) one. From a physical point of view, the inclusion of the long-range van der Waals interactions for the flat adsorption of pyridine on the Cu(110) surface modifies the nature of the adsorption process from physisorption to chemisorption.

### D. Electronic structure

In practice, three basic questions have to be answered in order to provide a clear picture of the bonding mechanism of a molecule on a surface: (i) which molecular orbitals are implied in the bonding process: (a) HOMOs, (b) LUMOs, or (c) HOMOs and LUMOs in a donation and back-donation bonding process; (ii) what is their position relative to the Fermi level of the metal surfaces; and (iii) in which way does the molecule-metal interaction affects the molecular orbitals,

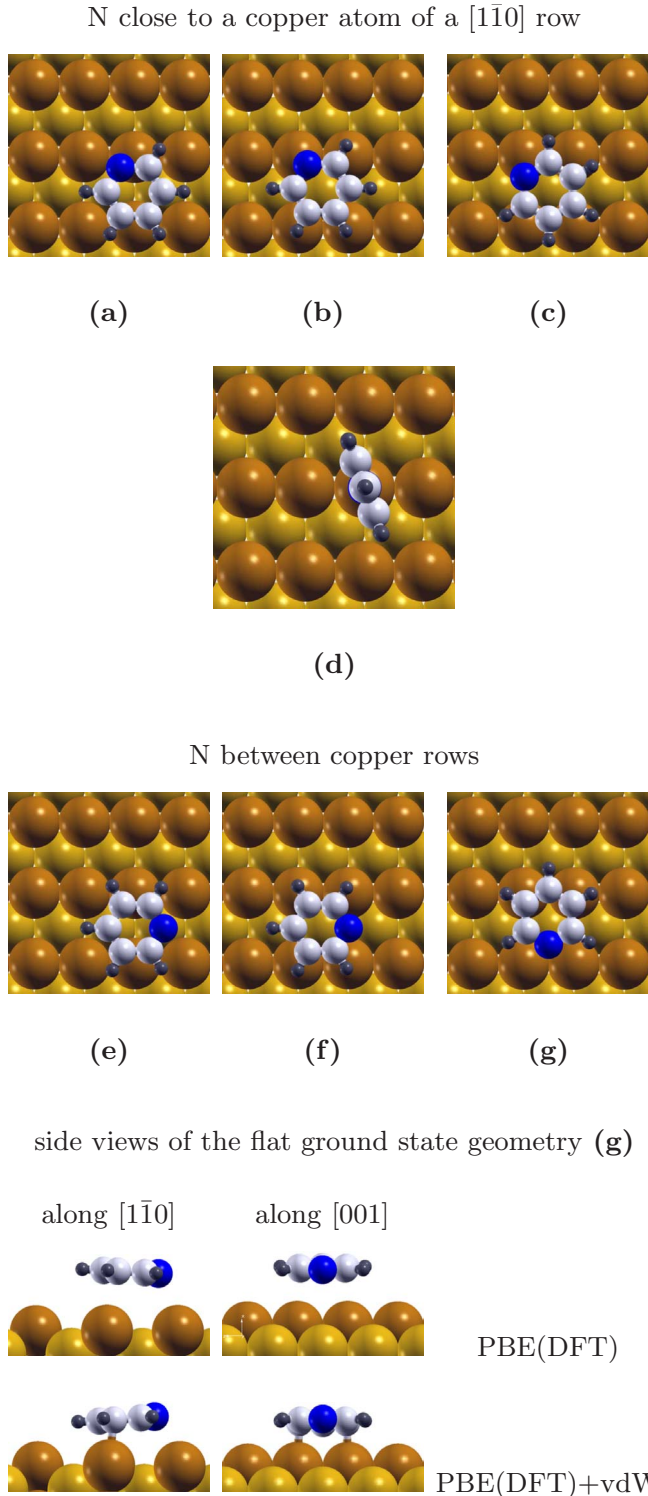


FIG. 4. (Color online) Several flat adsorption configurations of the pyridine molecule on Cu(110) and Ag(110) surfaces. The (a), (b), and (c) starting configurations with the N atom of the molecule close to a copper atom of a  $[1\bar{1}0]$  row relax to a local minimum geometry such that the pyridine is perpendicular to the metal surface as shown in (d). In the (e), (f), and (g) starting geometries the relaxed pyridine molecule remains flat on the surface. In this case the most stable local minimum corresponds to configuration (g) where the N atom is above two adjacent  $[001]$  rows.

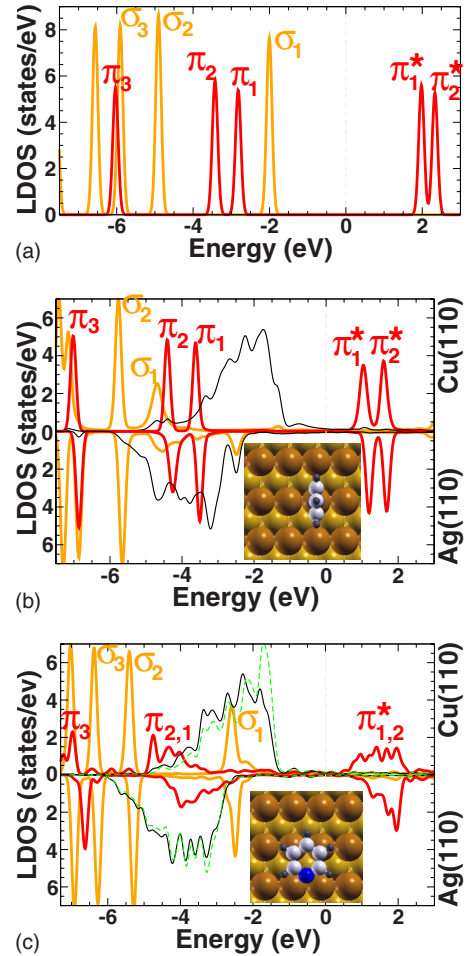


FIG. 5. (Color online) Local density of states (LDOS) calculated for the (a) gas phase, (b) perpendicular ( $[001]$  adsorption configuration; see Fig. 2), and (c) flat [see Fig. 4(g)] geometries of the pyridine molecule adsorbed on Cu(110) and Ag(110) surfaces. The thick red (thick black) line corresponds to the  $\pi$ -type electrons and the thick orange (thick gray) one corresponds to the  $\sigma$ -type electrons. For the flat adsorption geometry, the  $d$  bands of Cu underneath the C2 atom (C2 atom is equivalent to C4 atom) [see also Table I and Fig. 4(g)] are drawn with thin black lines while the  $d$  bands of the surface metal atom underneath the N atom are plotted with thin green (thin gray) lines. For (b) and (c) graphs, the upper and lower panels correspond to the Cu(110) and Ag(110) surfaces, respectively.

i.e., (a) are the orbitals slightly broadened and still keep their localized molecular character or (b) broad bands with mixed metallic and molecular character are formed.

In order to investigate the bonding mechanism of the pyridine on Cu(110) and Ag(110) surfaces we first identified the LDOS for the adsorbed molecule-substrate system by summing over all atomic contributions. The corresponding calculated LDOS for the perpendicular and flat adsorption are reported in Figs. 5(b) and 5(c), respectively. The energy range of interest for understanding the coupling of the  $C_5H_5N$  molecule to the Cu/Ag(110) surfaces through metal  $d$  bands is from  $-5.5$  to  $-1.0$  eV below Fermi level. Since in the case of the perpendicular adsorption geometry the structural changes induced by van der Waals corrections are neg-



ligible, in the following we will focus on the electronic structure obtained without these corrections. On the contrary, as such corrections are very important for the flat adsorption geometry its electronic structure is analyzed while taking into account these dispersion effects.

The analysis of LDOS for the perpendicular adsorption configuration reveals that in the case of both substrates, the bonding mechanism involves a strong hybridization of pyridine HOMO ( $\sigma_1$  orbital) and HOMO-2 ( $\pi_2$  orbital) (see Fig. 1) with the  $d_{y^2}$ - and  $d_{yz}$ -type orbitals of the substrate, respectively. The interaction of HOMO-1 ( $\pi_1$ ) with the  $d_{x^2-z^2}$ -type orbital is weaker and in consequence, this molecular orbital is not pushed as low in energy as compared to the HOMO ( $\sigma_1$ ) and HOMO-2 ( $\pi_2$ ). We would like to emphasize that HOMO-1 ( $\pi_1$ ) does not interact as strongly as HOMO-2 ( $\pi_2$ ) because it has no electron distribution on N atom. Therefore it is expected that its contribution to the N-metal binding is negligible, while HOMO-2 ( $\pi_2$ ) has a considerable amount of electron density on the N atom and interacts more effectively with the metal orbitals.

On the contrary, for the flat adsorption configuration, the LDOS analysis shows that the strong hybridization of HOMO-1 ( $\pi_1$ ) and HOMO-2 ( $\pi_2$ ) with the metal  $d$  states results in broad bands with mixed metallic and  $\pi$  molecular characters. The interaction of the pyridine HOMO ( $\sigma_1$ ) with the metal is much weaker, and in consequence this orbital remains localized mainly on the molecule.

As a general characteristic for both perpendicular and flat adsorption configurations, the lowest unoccupied molecular orbitals  $\pi_1^*$  and  $\pi_2^*$  or the antibonding band  $\pi_{1,2}$  [see Figs. 5(b) and 5(c), respectively] do not play a role in the bonding process since they remain unoccupied in the molecule-surface system. This is a clear proof that the pyridine-surface interaction has a strong covalent character. Indeed, if the LUMOs were partially or fully occupied then a strong ionic interaction between metal and molecule would take place.

However, there is a significant difference between the electronic structure of the pyridine on the Cu(110) surface with respect to that on the Ag(110) one. As already mentioned, for the perpendicular adsorption geometry the N-Cu bond length is much smaller than that of the N-Ag one. This structural detail is the first evidence that the  $C_5H_5N$ -Cu(110) surface interaction is much stronger than the  $C_5H_5N$ -Ag(110) one. A stronger molecule-substrate interaction for the  $C_5H_5N$ -Cu(110) system is also obvious from the analysis of its electronic structure. As presented in Fig. 5, the main bonding orbital ( $\sigma_1$ ) is pushed to much lower energies for the Cu surface (-4.7 eV) as compared to the Ag one (-2.5 eV). This effect can be understood starting from the observation that the  $d$  bands of the Cu(110) surface lie closer to Fermi level than those of the Ag(110) substrate. In a Schottky-Mott barrier model, this implies that the pyridine HOMO is closer in energy to the  $d$  bands of the Cu(110) substrate than those of the Ag(110) surface. In consequence, this molecular orbital interacts more strongly with the Cu(110) surface than with the Ag(110) one, leading to a larger energy splitting in the former case and thus to a larger adsorption energy for the  $C_5H_5N$  on the Cu(110) surface than on the Ag(110) one.

An intuitive chemical view of the nitrogen-metal-atom interaction is presented in Fig. 6. It shows that the interaction

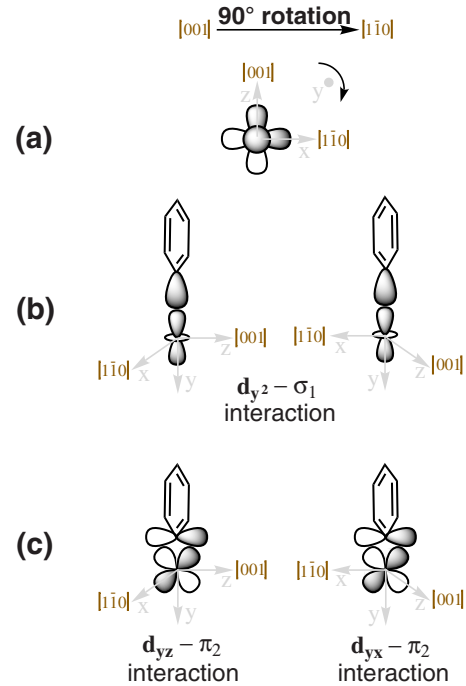


FIG. 6. (Color online) In a very simplified chemical model, the N-metal interaction for the perpendicular adsorption takes place via two types of bonds:  $\sigma$  and  $\pi$ . (a) Top view of the  $d_{y^2}$ ,  $d_{yz}$ , and  $d_{yx}$  orbitals located at the metal atom, binding the N atom of the  $C_5H_5N$  molecule. (b) The  $\sigma$ -type bond is formed along the  $y$  direction by a bonding overlap between  $d_{y^2}$  orbital of the metal and  $\sigma_1$  orbital of the pyridine. (c) The  $\pi$ -type bond is formed along the  $[001]$  ( $[1\bar{1}0]$ ) direction between  $d_{yz}$  ( $d_{yx}$ ) orbital of the metal with the  $\pi_2$  orbital of the pyridine molecule.

of the  $d_{y^2}$  orbital of the metal and the HOMO ( $\sigma_1$ ) orbital of the pyridine is independent of the molecular plane orientation. Moreover, the hybridizations along the  $[001]$  or  $[1\bar{1}0]$  directions between the  $d_{yz}$  or  $d_{yx}$  orbital of the metal surface and the HOMO-2 ( $\pi_2$ ) orbital are equivalent. So, within this simple model, it is expected that the total energies of the  $[001]$  and  $[1\bar{1}0]$  configurations are equal. In reality, this degeneracy is slightly shifted in the presence of the substrate due to a different surface environment when the molecular plane lies along the  $[001]$  or  $[1\bar{1}0]$  directions. Nevertheless, the rather small energy difference between these two perpendicular configurations indicates a strong local character of the interaction between the nitrogen and the surface metal atom.

As a characteristic of the copper surface, when rotating the molecular plane from  $[001]$  toward the  $[1\bar{1}0]$  direction, the overlap between  $d_{yz}$  and HOMO-2 ( $\pi_2$ ) will decrease and therefore the total energy of the system will increase (see Figs. 3 and 6). By further rotating the molecular plane toward  $[1\bar{1}0]$  the bonding overlap between  $d_{yx}$  and  $\pi_2$  starts to increase and therefore the total energy of the systems will decrease. Thus, the high energy barrier between the  $[001]$  and  $[1\bar{1}0]$  configurations shown in Fig. 3 indicates a strong  $d_{yz(yx)}-\pi_2$  interaction for the Cu(110) surface. On the contrary, the low energetic barrier in the case of Ag(110) surface shows that the  $d_{yz(yx)}-\pi_2$  interaction is quite weak and there-

fore the bonding takes place mostly through  $d_{y^2}$  orbital of the metal and the HOMO ( $\sigma_1$ ) orbital of the pyridine. Therefore, we can assume that, when the perpendicular adsorbed molecules are arranged in a closely packed self-assembled monolayer, the van der Waals intermolecular interactions will play the major role for the Ag(110) as compared to the Cu(110) surface.

For the flat adsorption geometry, due to the van der Waals interactions, the average molecule-surface distance is much smaller ( $\approx 0.5$  Å) for the Cu(110) as compared to the Ag(110) surface. As in the case of perpendicular adsorption geometry, this indicates a stronger interaction between the molecule and the copper surface. This effect is also easily seen in the LDOS characteristics in Fig. 5(c), which shows that the  $\pi_{1,2}$  bands are shifted lower in energy for the copper surface as compared to the silver one.

The basic features displayed by the LDOS of the  $C_5H_5N$  molecule on Cu/Ag(110) surfaces may be easily understood in terms of the Anderson-Newns model,<sup>38</sup> which describes the interaction of a localized molecular orbital with the metal states. In the case of a metal with a completely occupied  $d$  band (Cu and Ag), this model predicts that both bonding and antibonding molecular orbitals are formed, analog to the bonding and antibonding molecular orbitals formed by two interacting atoms. As shown already for other molecules, which use the carboxylate group to anchor to the Cu(110) surfaces,<sup>15,16</sup> [also in the case of the pyridine molecule adsorbed on the Cu(110) surface] an effective hybridization between molecule's HOMO with the  $d$  bands of the metal occurs and the bonding process can be seen as a chemisorption one. A schematic view of the pyridine interaction with Cu(110) or Ag(110) metal surfaces for the perpendicular and flat adsorption geometries in terms of this model is presented in Fig. 7(a) and 7(b), respectively.

#### IV. SUMMARY

In the present study we focused on an *ab initio* investigation of the adsorption mechanism of the pyridine ( $C_5H_5N$ ) on the Cu(110) and Ag(110) surfaces. The pyridine molecule can bind to these substrates via its nitrogen lone-pair electrons or through its planar  $\pi$ -like molecular orbital leading to a perpendicular or parallel adsorption geometry, respectively. Our first-principles calculations clearly show that, in the ground state, the heterocyclic ring of  $C_5H_5N$  is perpendicular to the Cu(110) and Ag(110) surfaces and it is aligned along the [001] surface direction. However, when starting with a parallel adsorption configuration, the geometry of the relaxed molecule-surface system depends significantly on the position of the N atom on the Cu(110) and Ag(110) surfaces. More specifically, when the N atom is placed close to a surface atom or above it, in the final relaxed geometry the heterocyclic ring of pyridine molecule is perpendicular to both surfaces. However, when the N atom is between the surface atoms, the molecule remains flat on these substrates. Since in the latter case the molecule-surface interactions take place through the planar aromatic  $\pi$ -like molecular orbital, we analyzed the role of the van der Waals interactions on the bonding process of pyridine on Cu(110) and Ag(110) surfaces by

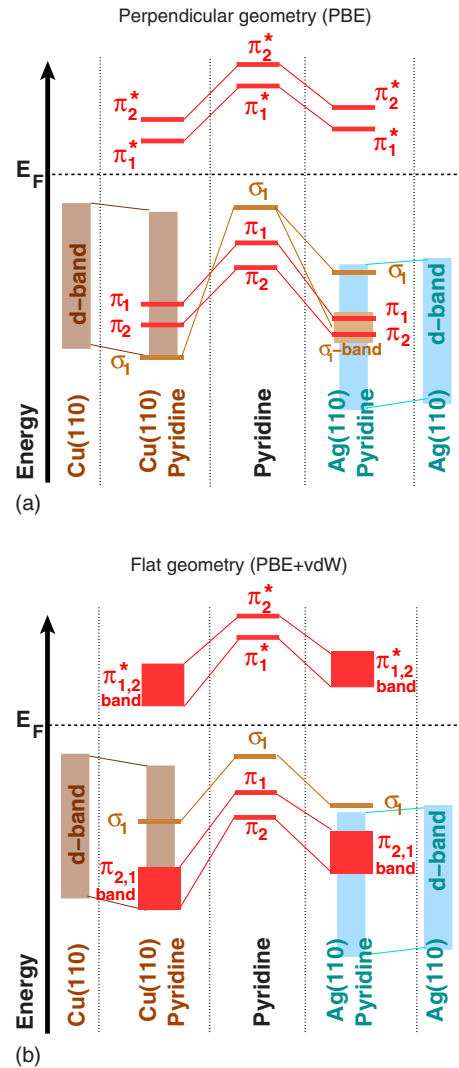


FIG. 7. (Color online) Schematic view of the hybridization of pyridine molecular orbitals with Cu(110) and Ag(110)  $d$  bands. (a) In the case of the perpendicular adsorption geometry, the pyridine molecule binds to surface mainly via the  $\sigma_1$  molecular orbital. For the Cu(110) surface this orbital is drastically shifted to lower energies, well below the  $\pi_1$  and  $\pi_2$  orbitals, while for the Ag(110) surface the  $\sigma_1$  orbital gives rise to a peak with small weight above the  $\pi_1$  and  $\pi_2$  orbitals and a broad  $\sigma$ -type bond having also a small intensity [see also Fig. 5(b)]. (b) In the flat adsorption geometry the strong hybridization of the  $\pi_1$  and  $\pi_2$  molecular orbitals with the metal  $d$  bands leads to the formation of broad bonding  $\pi_{2,1}$  and antibonding  $\pi_{1,2}^*$  bands with mixed  $\pi$  and metallic character. However, the shift toward lower energies of the occupied  $\pi_{2,1}$  band is larger for the copper than for the silver surface. This effect is due to a much stronger hybridization of the  $\pi$  molecular orbitals with the  $d$  bands of the metal surface in the former case [see also Fig. 5(c)].

employing a semiempirical method. We prove that the dispersion effects corresponding to the long-range van der Waals interactions play an important role from both geometrical and energetic point of views. In the case of the perpendicular adsorption configurations, the inclusion of van der Waals forces leads essentially to the same relaxed geometries, while a van der Waals-corrected energy functional (PBE+vdW) lowers the adsorption energy by  $\approx 0.2$  eV on



both surfaces. On the contrary, in the case of the parallel adsorption geometries, the van der Waals corrections have a substantial impact on the geometry of the relaxed configurations and on the corresponding adsorption energies. From the electronic structure point of view, for the ground-state perpendicular adsorption geometry, the interaction of the pyridine with the  $d$  bands of the metals results in a small broadening of the molecular orbitals—the most affected one being the HOMO ( $\sigma_1$ ). This is not the case for the most stable flat adsorption geometry, where the interaction of the HOMO  $-1(\pi_1)$  and HOMO  $-2(\pi_2)$  with the  $d$  bands of the metals results in broad bands with mixed  $\pi$  and metallic characters.

## ACKNOWLEDGMENTS

The computations were performed with the help of the JUMP and Blue/Gene supercomputers at the Forschungszentrum Jülich, Germany. We acknowledge the financial support from the DFG (Grants No. SPP1243 and No. HO 2237/3-1) and Japan Society for the Promotion of Science. V.C. and N.A. thank H. Hölscher, H. Fuchs (University of Münster), Y. Moriwaka (Osaka University), and K. Schroeder (Research Center Jülich) for many fruitful discussions and continuing support.

\*n.atodiresei@fz-juelich.de

- <sup>1</sup>N. Atodiresei, P. H. Dederichs, Y. Mokrousov, L. Bergqvist, G. Bihlmayer, and S. Blügel, *Phys. Rev. Lett.* **100**, 117207 (2008).
- <sup>2</sup>C. D. Dimitrakopoulos, S. Purushothaman, J. Kymissis, A. Callegari, and J. M. Shaw, *Science* **283**, 822 (1999).
- <sup>3</sup>C. Dimitrakopoulos and P. Malenfant, *Adv. Mater. (Weinheim, Ger.)* **14**, 99 (2002).
- <sup>4</sup>V. C. Sundar, J. Zaumseil, V. Podzorov, E. Menard, R. L. Willett, T. Someya, M. E. Gershenson, and J. A. Rogers, *Science* **303**, 1644 (2004).
- <sup>5</sup>J. E. Green *et al.*, *Nature (London)* **445**, 414 (2007).
- <sup>6</sup>F. Schreiber, *Prog. Surf. Sci.* **65**, 151 (2000).
- <sup>7</sup>M. A. Reed, C. Zhou, C. J. Muller, T. P. Burgin, and J. M. Tour, *Science* **278**, 252 (1997).
- <sup>8</sup>J. Chen, M. A. Reed, A. M. Rawlett, and J. M. Tour, *Science* **286**, 1550 (1999).
- <sup>9</sup>M. A. Reed, J. Chen, A. M. Rawlett, D. W. Price, and J. M. Tour, *Appl. Phys. Lett.* **78**, 3735 (2001).
- <sup>10</sup>J. Park, J. I. G. Abhay, N. Pasupathy, C. Chang, Y. Yaish, J. R. Petta, M. Rinkoski, J. P. Sethna, H. D. Abruña, P. L. McEuen, and D. C. Ralph, *Nature (London)* **417**, 722 (2002).
- <sup>11</sup>G. Heimel, L. Romaner, J.-L. Brédas, and E. Zojer, *Phys. Rev. Lett.* **96**, 196806 (2006).
- <sup>12</sup>G. Heimel, L. Romaner, J.-L. Brédas, and E. Zojer, *Surf. Sci.* **600**, 4548 (2006).
- <sup>13</sup>G. Heimel, L. Romaner, E. Zojer, and J.-L. Brédas, *Nano Lett.* **7**, 932 (2007).
- <sup>14</sup>B. Frederick, F. Leibsle, S. Haq, and N. V. Richardson, *Surf. Rev. Lett.* **3**, 1523 (1996).
- <sup>15</sup>N. Atodiresei, K. Schroeder, and S. Blügel, *Phys. Rev. B* **75**, 115407 (2007).
- <sup>16</sup>N. Atodiresei, V. Caciuc, K. Schroeder, and S. Blügel, *Phys. Rev. B* **76**, 115433 (2007).
- <sup>17</sup>A. Bilić, J. R. Reimers, and N. S. Hush, *J. Phys. Chem. B* **106**, 6740 (2002).
- <sup>18</sup>H. Lesnard, M.-L. Bocquet, and N. Lorente, *J. Am. Chem. Soc.* **129**, 4298 (2007).
- <sup>19</sup>D. B. Dougherty, J. Lee, and J. J. T. Yates, *J. Phys. Chem. B* **110**, 11991 (2006).
- <sup>20</sup>B. L. Rogers, J. G. Shapter, and M. J. Ford, *Surf. Sci.* **548**, 29 (2004).
- <sup>21</sup>N. Atodiresei, V. Caciuc, S. Blügel, and H. Hölscher, *Phys. Rev. B* **77**, 153408 (2008).
- <sup>22</sup>J. R. Hahn and W. Ho, *J. Chem. Phys.* **124**, 204708 (2006).
- <sup>23</sup>J.-G. Lee, J. Ahner, and J. J. T. Yates, *J. Chem. Phys.* **114**, 1414 (2001).
- <sup>24</sup>J. Lee, I. A. Balabin, D. N. Beratan, J.-G. Lee, J. John, and T. Yates, *Chem. Phys. Lett.* **412**, 171 (2005).
- <sup>25</sup>P. Hohenberg and W. Kohn, *Phys. Rev.* **136**, B864 (1964).
- <sup>26</sup>G. Kresse and J. Hafner, *Phys. Rev. B* **47**, 558 (1993).
- <sup>27</sup>G. Kresse and J. Furthmüller, *Phys. Rev. B* **54**, 11169 (1996).
- <sup>28</sup>P. E. Blöchl, *Phys. Rev. B* **50**, 17953 (1994).
- <sup>29</sup>G. Kresse and D. Joubert, *Phys. Rev. B* **59**, 1758 (1999).
- <sup>30</sup>J. P. Perdew, K. Burke, and M. Ernzerhof, *Phys. Rev. Lett.* **77**, 3865 (1996).
- <sup>31</sup>G. Makov and M. C. Payne, *Phys. Rev. B* **51**, 4014 (1995).
- <sup>32</sup>S. Grimme, *J. Comput. Chem.* **27**, 1787 (2006).
- <sup>33</sup>F. Ortmann, W. G. Schmidt, and F. Bechstedt, *Phys. Rev. Lett.* **95**, 186101 (2005).
- <sup>34</sup>F. Ortmann, F. Bechstedt, and W. G. Schmidt, *Phys. Rev. B* **73**, 205101 (2006).
- <sup>35</sup>K. K. Innes, I. G. Ross, and W. R. Moomaw, *J. Mol. Spectrosc.* **132**, 492 (1988).
- <sup>36</sup>J. B. Martins and T. A. Fialho, *J. Mol. Struct.: THEOCHEM* **732**, 1 (2005).
- <sup>37</sup>U. D. Priyakumar, T. C. Dinadayalane, and G. N. Sastry, *Chem. Phys. Lett.* **337**, 361 (2001).
- <sup>38</sup>B. Hammer and J. K. Nørskov, *Chemisorption and Reactivity of Supported Clusters and Thin Films* (Kluwer, Dordrecht, 1997).